

the modulation between 0 V and -4.3 V, in light of chirp and saturation considerations. The first mode of operation yields slightly negative chirp, whereas the second yields positive chirp. The optical saturation and carrier accumulation effects are much weaker in the first due to reduced coupling between optical fields and excitons, and due to more effective carrier sweep-out.

We performed a high-speed modulation test of the uncoated modulator by using an HP8703A and utilizing an optical circulator to extract modulated light from the AFPM. Figure 2 shows frequency responses of modulators of three different sizes. The frequency response shows an instrument-limited modulation bandwidth of 20 GHz for an 18- μm -diameter device. We utilized a 40- μm -diameter dielectric coated device bias point at -7 V to investigate large signal modulation characteristics. Figures 3 (a) and (b), show eye diagrams of the modulated signal at 2.488 Gbit/s and 9.9532 Gbit/s with $2^{31}-1$ PRBS. The 2.488 Gbit/s eye diagram is clear, whereas the 9.9532 Gbit/s eye diagram shows a degradation due to RF reflection (Fig. 3(c)). The 9.9532 Gbit/s bit pattern, however, indicates no degradation due to a bandwidth limit, and a use of a probe with an improved impedance matching is being pursued.

In conclusion, we have demonstrated 1.5- μm asymmetric Fabry-Perot modulators with bandwidths exceeding 20 GHz. The low insertion loss, high extinction ratio, and a large modulation bandwidth of the modulator imply a potential for widespread applications in future high-speed optical communication systems.

1. R. H. Yan, R. J. Simes, and L. A. Coldren, *IEEE Photon. Technol. Lett.* **1**, 273 (1989).
2. C. C. Barron, C. J. Mahon, B. J. Thibeault, G. Wang, J. R. Karin, L. A. Coldren, and J. E. Bowers, *DRC, Late News Papers VIB-9* (1993).
3. S. J. B. Yoo, R. Bhat, A. Scherer, K. Uomi, C. E. Zah, M. A. Koza, M. C. Wang, and T. P. Lee, in *LEOS '92*, (1992), post-deadline paper PD-6.

TuC2

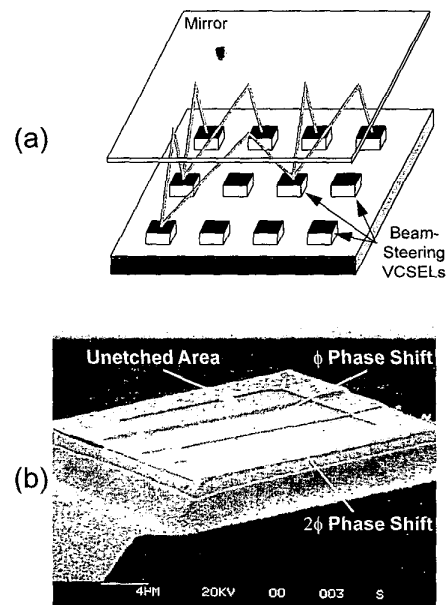
11:15 am

4 × 4 reconfigurable optical interconnection network using beam-steering vertical-cavity surface-emitting lasers

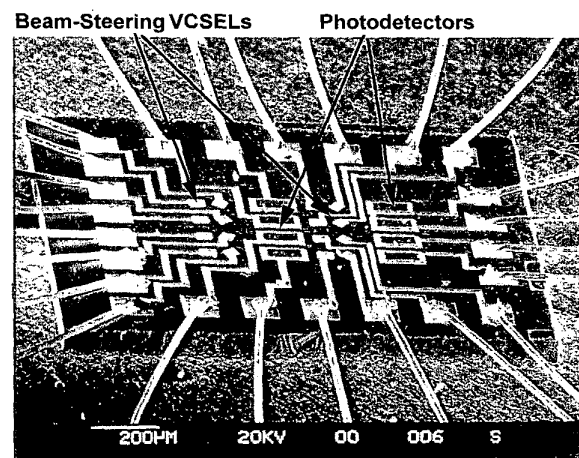
L. Fan, M. C. Wu, H. C. Lee,* P. Grodzinski,* *UCLA, Electrical Engineering Department*

Free-space optical interconnect¹ employing vertical-cavity surface-emitting lasers (VCSEL) can significantly improve the performance of massively parallel processors. Recently, we have reported a novel beam-steering VCSEL that could switch the direction of the output beam. Beam-steering angles from 2.6° to 9.6° have been reported.² Such beam-steering VCSELs are particularly suitable for implementing multistage space-division switching networks such as banyan networks. Different interconnection paths can be setup by selecting different beam directions. In this paper, we report on novel 4×4 reconfigurable optical interconnection network using a monolithic array of beam-steering VCSELs and photodetectors.

The schematic structure of the single-chip photonic banyan network is illustrated in Fig. 1(a). It consists of two parts: a



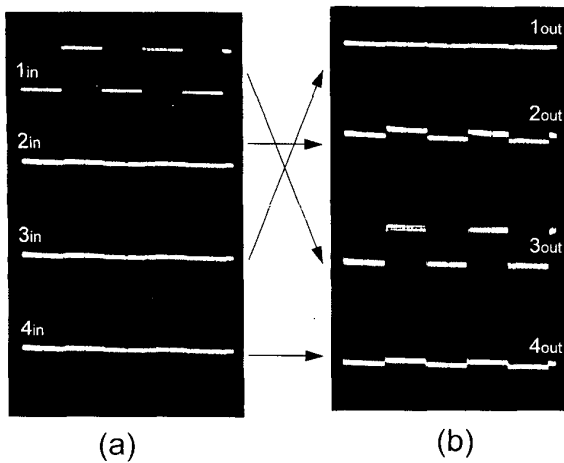
TuC2 Fig. 1. (a) The schematic diagram of the 4×4 monolithic photonic banyan network. (b) The SEM photograph of the beam-steering VCSELs with integrated optical beam router. The three-step phase-shifter is realized by selectively etching the top layer of VCSEL.



TuC2 Fig. 2. The SEM photograph of a packaged 4×4 photonic banyan network.

monolithic switching fabric that contains all the active optoelectronic devices and electronic circuits; and an external plane mirror to bend the optical beams back to the switching fabric. Each switching element, or pixel, consists of a photodetector and two beam-steering VCSELs. Because the optical beam router is already integrated on the VCSEL, no additional passive optical elements are needed.

Figure 1(b) shows the scanning electron micrograph (SEM) of the beam-steering VCSEL with a three-step optical beam router. The beam router is created by multiple etching on the surface of VCSEL. To avoid interfering the VCSEL operation or introduction of high-order modes, each step is designed to be half-wavelength high so that the reflectivity of the top distrib-



TuC2 Fig. 3. The switching performance of the photonic banyan network. (a) Signals of the four input channels, and (b) signals of the four output channels. The signal in channel 1 has been routed to channel 3 at output stage.

uted Bragg reflector (DBR) remains uniform. The resulting steering angle of the VCSEL is equal to $\theta = \sin^{-1}(\lambda/2\pi d(1 - 1/n))$, where λ is the free-space wavelength and n is the refractive index of the phase-shifter. The steering angle can be varied by changing the spacing d between the phase-shifters.

Figure 2 shows the SEM micrograph of the packaged 4×4 photonic banyan chip. For testing purpose, all VCSELs and photodetectors are connected to bonding pads on the peripheral so that they can be evaluated independently. The photonic banyan chip is packaged using a standard DIP IC package. The external mirror is realized by replacing cap of the IC package with a gold-coated mirror. Because only a plane mirror is required for external optics, no lateral optical alignment is required. The routing angles of each VCSEL has been precisely defined by photolithographic process. The switching performance of banyan network has also be characterized. Figure 3(a) shows the signals of the four input channels. Channel 1 is modulated by a square wave. After passing through the 4×4 banyan network, the signal is routed to channel 3 of the output terminals, as shown in Fig. 3(b). The small cross talk in the adjacent channels can be further reduced by decreasing the beam divergence angles (3.3° in current design) of VCSELs.

In conclusion, a monolithically integrated 4×4 reconfigurable optical interconnection network has been demonstrated using arrays of beam-steering VCSELs. This approach eliminates the need of bulk optical components and critical alignment, and can greatly reduce the volume of optical interconnect for massively parallel processors.

1. S. H. Lee, V. H. Oziguz, J. Fan, D. Zaleta, and C. K. Cheng, "Computer aided design and packaging optoelectronic systems with free space optical interconnects," in *Proc. IEEE Custom Integrated Circuits Conference*, 1993, pp. 29.3.1-29.3.4.
2. L. Fan, M. C. Wu, H. C. Lee, and P. Grodzinski, "Novel vertical cavity surface-emitting lasers with integrated optical beam router," *Electron. Lett.* **31**, 729-730 (1995).

*Motorola Inc. Phoenix Corporate Research Laboratories

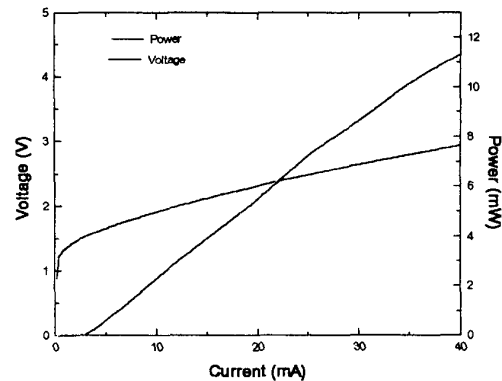
TuC3 (Invited)

11:30 am

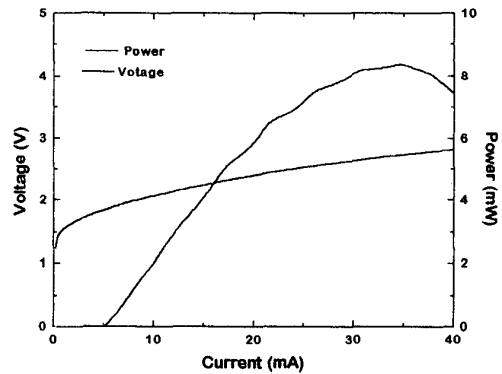
Surface-emitting laser for interconnects

M. R. T. Tan, S. W. Corzine, R. P. Schneider, Y. M. Houng, K. H. Hahn, T. C. Huang, S. Y. Wang, J. Dudley,* *Hewlett Packard Laboratories, 3500 Deer Creek Road, Palo Alto, California 94304*

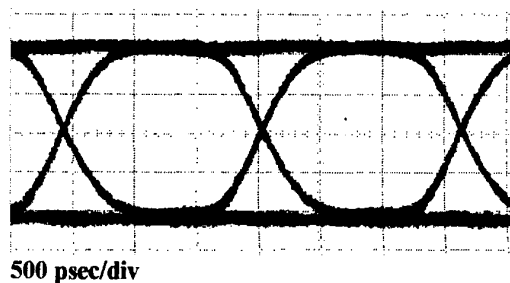
Multimode optical fiber data links have traditionally used light-emitting diodes (LED) as the optical source. The LED is an ideal source for most applications, but as data rate increases, it becomes increasing necessary to find another "LED-like" de-



TuC3 Fig. 1. LI and IV characteristic of 24-µm-diameter 980-nm VCSEL.



TuC3 Fig. 2. LI and IV characteristics of 15-µm-diameter 850-nm VCSEL.



TuC3 Fig. 3. Eye diagram at 622 Mbps with 2^7-1 PRBS for a 24-µm-diameter 980-nm VCSEL.